Coherent Change Detection with SAR

Patricia Wright, Trevor Macklin, Chris Willis, and Tony Rye
BAE SYSTEMS, Advanced Technology Centre,
Great Baddow, Chelmsford, Essex CM2 8HN, UK.

Abstract - **In the context of investigating coherent SAR data for battle damage assessment, we examine the ability to detect changes in objects using synthetic-aperture radar (SAR) observations. The emphasis is on targets which are a few resolution cells in extent. Both coherent and non-coherent methods are studied. Coherent methods are effective when clutter coherence is high. The correlation between intensity images may also be used to detect changes. Practical performance limits are set by sources of phase noise, such as the temporal coherence of clutter, and the spatial resolution of the sensor compared with the target/change dimensions.**

Keywords: change detection, SAR, coherence.

I Introduction

The ability to detect change in targets using remote surveillance is important for the assessment of damage caused by military operations. Synthetic-aperture radar (SAR) is an attractive tool for this application, because of its ability to collect fine resolution imagery in all illumination and weather conditions, while remaining distant from hostile action. Here we examine targets which are a few resolution cells in extent. Both coherent and non-coherent methods have been studied. The former exploit interferometric measurements (InSAR): pairs of complex SAR images are interfered, and the information is analysed for evidence of change. The latter uses the correlation between intensity images as a substitute for the interferogram coherence.

II Data Sets Reported

Both airborne and spaceborne SAR observations are studied, covering spatial resolutions of about 2-20m, and temporal baselines from 12.5 mins to 420 days. Two test sites are described here, an agricultural site at Monks Wood (UK), imaged in 2000, and Athens, covering the construction work for the 2004 Olympic Games. The properties of these data sets are summarised below.

Site	Time lag	Sensor (GHz)	Incident angle	Resolution range x azimuth
Monks Wood	12.5 min	E-SAR (1.3)	25°-58°	2 m ground range x 3 m
Athens	24 hrs 420 days	ERS & ASAR (5.3)	19°-26°	20 m ground range x 4 m

III Fundamental Theory

The fundamental quantity of interest is coherence, γ, which is defined by:

$$\gamma = \frac{\left\langle s_1 s_2^* \right\rangle}{\sqrt{\left\langle s_1 s_1^* \right\rangle \left\langle s_2 s_2^* \right\rangle}}$$

where s_1 and s_2 are the complex amplitudes measured on two passes over the site of interest, and the angular brackets denote expectation values. In order to reduce the noise and the bias on the estimated coherence, γ has to be constructed from multi-looked data [1]. The image of coherence is therefore obtained at a coarser spatial resolution to that of the original single-look data.

An equivalent of the coherence may be calculated from the correlation coefficient between detected images. [2] proposes that γ may be estimated from the correlation coefficient ρ between detected images, using the following relation:

$$\rho = (1 + \gamma^2) / 2$$

Hence γ is set to zero if ρ is less than 0.5. This is an example of the Siegert relation which follows from the gaussian statistics of complex SAR imagery of natural scenes. The basic assumptions are that there are many scatterers per resolution cell, that no individual scatterers dominate over the others, and that the spatial correlation between scatterers is less than the spatial resolution of the SAR. Hence the method should work well over most natural scenes. We have previously used this relation in analysis of speckle filtering using complex SAR data [3] and found that it worked well over both ocean and land scenes.

IV Results: Monks Wood

The Monks Wood data (Figures 1 and 2) show clear detection of change in the positions of small targets. In the coherence images, high coherence

is indicated by white. Change of position is evidenced by pairs of "holes" in the coherence map, where the coherence has dropped by 0.4-0.5 compared to the clutter. The high coherence clutter makes detection of change relatively easy. However, even with the short time lag of 12.5min, forest areas and some field boundaries have relatively low coherence. This would produce some false-alarm detections if the user did not have prior information about the location of vegetated regions. It is expected that such false alarms would be more common at higher frequencies, which are more sensitive to change in surface scatterers due to environmental effects.

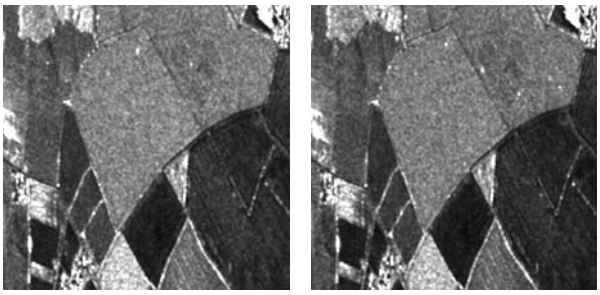

Figure 1 Left: first image of Monks Wood; right: second image, 12.5 min later.

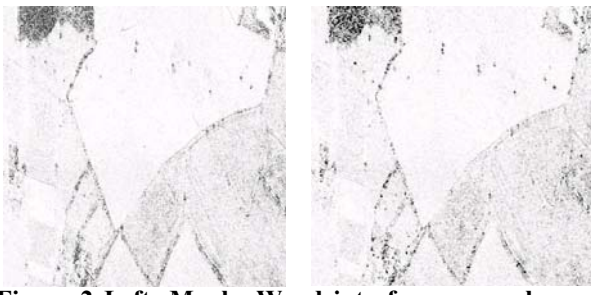

Figure 2 Left: Monks Wood interferogram coherence; right: correlation coefficient of image intensities converted to a coherence

V Results: Athens

Small changes in the positions of ships anchored in the Bay of Eleusis, north west of Athens, are detected using spaceborne data with a time lag of 24 hours (Figure 3). More extensive smoothing of data is required than that used for Monks Wood, because the ocean clutter is incoherent for this time lag. These small changes in ship position (~ 10 m) are comparable to the changes which would be associated with damage to individual buildings in a military operation.

Over non-forested land areas, coherence at C-band with a 24 hour time lag is quite high: the mean is about 0.65. However, it should be noted that coherence is low for regions of layover. This is caused by multiple backscatter signals being placed in the same range bin, thus destroying the phase signature of the data. At grazing incidence, shadowing would be expected to be a more significant factor than layover.

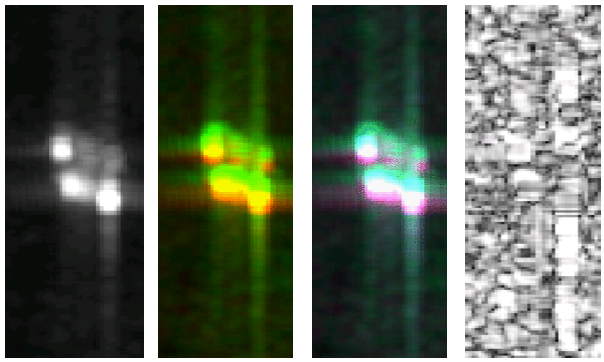

Figure 3 Ships, left to right: InSAR amplitude, composite (red: 1 Oct, green: 2 Oct), composite with InSAR amplitude (blue), and coherence.

Changes over several Olympic stadia are also detected with a time lag of 420 days. An example of the main Olympic Complex is shown in Figure 4. The optical imagery illustrates the changes that occurred over the period 2003 - 2004. The coherence shows total decorrelation over areas of significant change, while structures known to be unchanged (as indicated in the figure) remain coherent. A profile (taken along the yellow line in Figure 4) of the backscatter and coherent data is shown in Figure 5.

The profile shows a decrease in coherence to below 0.1 over areas of stadium construction. This is a decrease in coherence of around 0.15 compared to the more coherent regions around the Complex. Notice, however, that many regions not immediately associated with construction are also incoherent. Some of these are areas of vegetation, as previously observed in the Monks Wood data. Positive identification of change due to damage will require additional information, such as target location and clutter background identification.

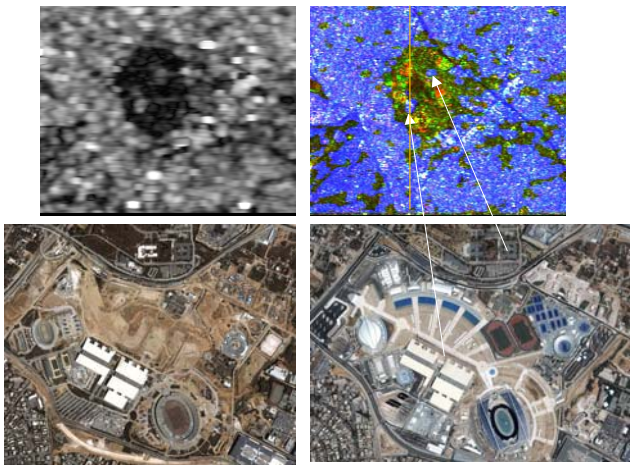

Figure 4 Top l: coherence image of the Olympic complex, Athens; top r: composite 2004 (red), 2003 (green) coherence above 0.12 (blue). A profile along the vertical yellow line is shown below. Bottom optical image 2003(l), optical image 2004(r). The arrows indicate areas unchanged over time.

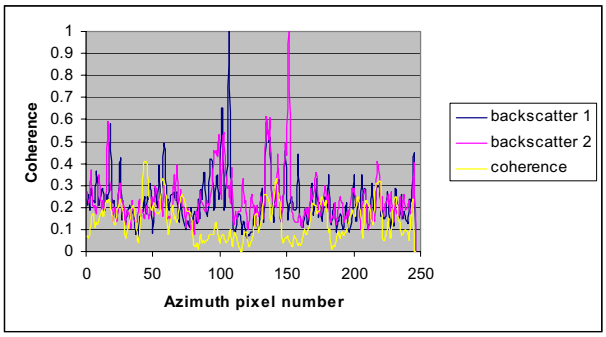

Figure 5 Coherence and backscatter profile

VI Statistics of image coherence

The statistical distribution of the clutter coherence may be modelled approximately using the Fisher z-transformation:

$$z = \frac{1}{2}\ln\left(\frac{1+\gamma}{1-\gamma}\right)$$

This has the advantage of transforming to a statistic which is approximately normally distributed [4], thus simplifying the computation of thresholds and false-alarm rates. The ability to detect a resolved target in coherence data may then be expressed by the following quantity Δ:

$$\Delta = \frac{z_b - z_t}{\sqrt{V_t + V_b}}$$

Here the subscripts t and b refer to the target and background, respectively. V_t and V_b are the corresponding variances in z_t and z_b. Both variances have the approximate value $1/(L\text{-}1)$, where L is the number of looks [4]. Hence Δ is the number of standard deviations by which the target differs from the background. Here we ignore the contribution of the background to the target signal.

For the purposes of illustrative calculation, we assume that $\Delta>3$ is required in order to provide a detection which is statistically significant. Different values of Δ may be obtained by changing the number of looks. In practice, higher values of Δ might be required if the user wants a small number of false alarms over a large area. Lower values of Δ may be acceptable if the user has already chosen a small area of interest and wants to maintain a spatial resolution which is as fine as possible in the coherence. From the Central Limit theorem, it follows that Δ is normally distributed with unit variance in the limit of a large number of looks, under the null hypothesis where the target has the same statistics as the background. Hence $\Delta>3$ occurs with probability 0.00135 if the null hypothesis is true.

The spatial resolution in the multi-look data should be no coarser than the size of the smallest targets of interest, typically 5m. Hence the number of looks defines the single look spatial resolution which is required in order to detect the target. The following table gives the number of looks required for various values of the mean coherence of the target and the background. Alternatively, we may start with a given single-look resolution and ask what difference in the coherence may be detected over a 5m x 5m area, with $\Delta>3$. The single-look spatial resolution required to detect a target whose coherence is 0.1 less than the clutter is shown in Figure 6.

Note that the single-look resolution is relatively insensitive to the clutter coherence once it is less than about 0.6. This means that we cannot use a coarser single-look spatial resolution than about 20cm unless we can guarantee that the clutter coherence will remain high.

Background coherence γ_b	Target coherence γ_t	No. of looks for $\Delta = 3$	Single-look spatial resolution if multi-look resolution is 5 m
0.99	0.8 0.4	8.5 4.6	1.7 m 2.3 m
0.9	0.8 0.4	128 17	0.4 m 1.2 m
0.8	0.8 0.4	Not detectable 41	Not detectable 0.8 m

Example of smoothing required for Δ>3 with different values of γ_t and γ

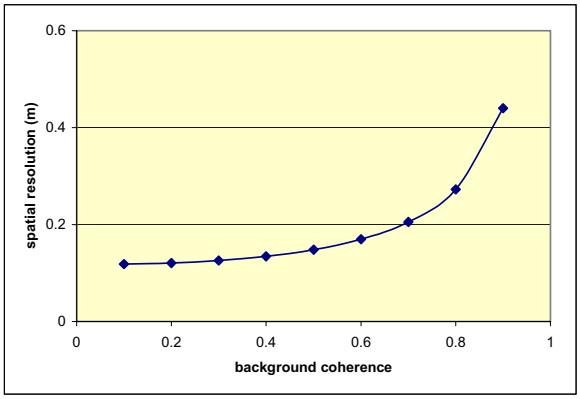

Figure 6 Spatial resolution required to detect a target with coherence 0.1 less than the clutter, at significance level $\Delta = 3$.

VII Conclusions

A number of important points for military applications arise from this analysis. Qualitatively, we may expect increased damage to be associated with a greater loss (in terms of magnitude and extent) of coherence in the relevant targets. This means that (ignoring dependences on other factors such as the target size relative to spatial resolution) targets with greatest damage are easier to detect when the background coherence is high. Undamaged targets will be easier to detect when the background coherence is low. Small changes in target position (relative to the target dimensions) may also be detected in the coherence. The coherence properties of the clutter are expected to depend on environmental parameters, including wind and rain, because of their effects on the motion and dielectric properties of scatterers in vegetation and terrain. Some clutter types, such as field boundaries can produce 'false alarm' detections. Contextual information may be needed to resolve some of these cases.

We have noted that the amount of smoothing required to detect statistically significant changes in coherence is an issue. The required smoothing becomes more extensive as the coherence of the clutter reduces. For clutter coherence close to 1 (Monks Wood) we found that the change in coherence over targets was readily detectable when the spatial resolution was degraded by a factor of 2.5 - 5 in each dimension. For clutter coherence close to 0 (ships in the Bay of Eleusis) we found that a degradation of the spatial resolution by a factor of at least 8 was required. This is consistent with the above statistical analysis, although we have not imposed a specific false-alarm rate in our data analysis.

References

1 Touzi, R et al., 1999, "Coherence estimation for SAR imagery", IEEE Trans. Geosci. Rem. Sems. **GE-37**, 135-149.

2 Monte Guarnieri, A and Prati, C, 1997,"A 'quick and dirty' coherence estimator for data browsing", IEEE Trans. Geosci. Rem. Sems. **GE-35**, 660-669.

3 Cordey, RA and Macklin, JT, 1989, "Complex SAR imagery and speckle filtering for wave imaging", IEEE Trans. Geosci. Rem. Sens. **GE-27**, 666-673.

4 Kendall, MG and Stuart, A, 1977, The Advanced Theory of Statistics, **Vol. 1**, 4th Edition, Griffin & Co.

Acknowledgement

The work reported in this paper was funded by the Electro-Magnetic Remote Sensing (EMRS) Defence Technology Centre, established by the UK Ministry of Defence and run by a consortium of BAE Systems Avionics, Thales Defence, Roke Manor Research and Filtronic.